

SUPPLEMENTAL INFORMATION FOR
E1 of α -Ketoglutarate Dehydrogenase Defends *Mycobacterium tuberculosis*
Against Glutamate Anaplerosis and Nitroxidative Stress

Christina Maksymiuk^{1,2}, Anand Balakrishnan^{1,2}, Ruslana Bryk¹, Kyu Rhee³ and Carl Nathan^{1,4}

¹Department of Microbiology and Immunology and ³Department of Medicine, Weill Cornell Medical College, New York, New York USA 10065

²Contributed equally

⁴To whom correspondence should be addressed at: cnathan@med.cornell.edu

Supplementary Figure Legends

Figure S1. HOAS participates in major metabolic and regulatory pathways in Mtb (A) Situation of HOAS and KDHC in Mtb tricarboxylic acid (TCA) cycle. GABA shunt, an alternate route from α -KG to succinate is shown as dotted line. (B) HOAS and KDHC are situated at the node of carbon and nitrogen metabolism. GarA controls glutamate metabolism.

Figure S2. Confirmation of *hoas* deletion and complementation of protein levels. (A) Southern blot design of Mtb genomic region with (I) native *hoas* (II) and the hygromycin resistance cassette after *hoas*' replacement. (B) Southern blot of digested Mtb DNA showing expected bands in $\Delta hoas$ candidates (Lanes 1-3) compared to WT (Lane 4). (C) Immunoblot analysis of HOAS protein in lysates from WT, $\Delta hoas$, $\Delta hoas::hoas$, $\Delta hoas::E956Ahoas$, and $\Delta hoas::E1038Ahoas$ using antiserum against KGD (here called HOAS). Antiserum against Dlat was used as a loading control.

Figure S3. Kinetic characterization of HOAS mutants. (A) Michaelis Menten plot for 2-ketoglutarate decarboxylase activity of WT and E956A HOAS in the presence and absence of AcCoA (200 μ M) determined by ferricyanide reductase assay described in methods. (B) Effect of allosteric regulator, AcCoA (0-1000 μ M), on 2-ketoglutarate decarboxylase activity of WT and E1038A HOAS determined by ferricyanide reductase assay. (Inset) Michaelis-Menten plot for E1038A HOAS. Data points are averages of triplicates and error bars are standard deviation. Results are representative of at least three independent experiments. AcCoA allosteric regulation data were fit to equations described in ref. 16.

Figure S4. HOAS is dispensible for growth in glycerol or acetate. Growth curves of H37Rv WT, deletion mutant ($\Delta hoas$), full length complement ($\Delta hoas::hoas$), and catalytically inactive mutant ($\Delta hoas::E956Ahoas$) in a modified Sauton's minimal medium (SMM) supplemented with either (A) glycerol, (B) acetate, each at 0.2%. Data are from one experiment representative of three.

Figure S5. Mtb requires HOAS activity to persist in mice. (A) Pathology of lungs infected with WT, $\Delta hoas$, $\Delta hoas::hoas$, and $\Delta hoas::E956Ahoas$ at 217 days post infection. (B) Bacterial burden in spleens of mice infected with WT, $\Delta hoas$, $\Delta hoas::hoas$, and $\Delta hoas::E956Ahoas$. Data are means \pm SD of for five mice per time point in one experiment representative of two, except that four mice were studied on day 1 and one mouse infected with $\Delta hoas::hoas$ died before day 217.

Figure S6. Metabolism of [^{13}C , ^{15}N] glutamate. (A) Uptake of [^{13}C , ^{15}N] glutamate. Data are means \pm SD (B) Abundance of ^{13}C -labeled central carbon metabolites. Data are from one experiment representative of at least two.

Figure S7. Dlat is essential for growth in glutamate. (A) Growth of $\Delta dlat$ in Sauton's minimal medium containing acetate (0.2%), glutamate (0.2%), or glycerol (0.2%). (B) Survival of $\Delta dlat$ in glutamate (0.2%). All data are means \pm SD of triplicates (C) Growth of $\Delta pdhC$ in Sauton's minimal medium containing acetate (0.2%), glutamate (0.2%), or glycerol (0.2%). Results are representative of at least two independent experiments.

Figure S8. Effect of glutamate on growth of $\Delta hoas::E1038Ahoas$ and $\Delta dlat$ Mtb strains. Mid-growth phase OD of (A) $\Delta hoas::E1038Ahoas$ in Sauton's minimal medium containing glycerol as the sole carbon source with varying amounts of additional glutamate; (B) $\Delta dlat$ in Sauton's minimal medium containing glycerol as the sole carbon source with varying amounts of additional glutamate All results are representative of at least two independent experiments.

Figure S9. Rapid Fire Mass spectrometric detection and characterization of KDH reaction. (a) EIC spectra at $m/z = 866.12$ showing succinyl CoA formation in the KDH reaction progress curve. First 3 sets

are standard curve, next 6 sets are KGDH reaction, next 6 sets are reaction without 2-ketoglutarate, and next 6 sets are reaction without NAD⁺. (b) Zoomed in version on the first set of peaks showing time course of reaction progress. First 6 samples are the unactivated and next 6 are the activated reaction. (c) Comparison of natural abundance isotopic distribution of standard and product. (d) EIC at m/z = 866.12 for the Michaelis-Menten kinetics reaction. (e) Zoomed in version on set of peaks (unactivated and activated) obtained with various concentrations of 2-ketoglutarate as indicated.

Figure S10. Kinetic characterization of KDH reaction. (a) Progress curves of activated (open symbols) and unactivated (filled symbols) KDH reaction (circles) and absence of 2-ketoglutarate (triangles) or absence of NAD⁺ (squares). (b) Michaelis Menten plot of 2-ketoglutarate for activated (open circles) and unactivated (filled circles) reaction. (c) Michaelis Menten plot of CoA for activated (open circles) and unactivated (filled circles) reaction. (d) Michaelis Menten plot of NAD⁺ for activated (open circles) and unactivated (filled circles) reaction. The fitted kinetic parameters are summarized in Table 1. Data points are averages of experimental triplicates and error bars are standard deviation. Solid lines in (a) are spline curves and in (b, c, and d) are regression fit to equation 1. Each experiment was repeated at least 3 times.

Figure S11. Mtb metabolome upon loss of KDHC function under various growth conditions. (A) Quantitation of intracellular metabolites with major changes when exposed to glutamate (0.05%) and acetate (0.2%) in Sauton's minimal medium. Quantitation of secreted metabolites with major changes when Mtb strains were exposed to (B) glycerol (0.2%) or (C) glutamate (0.2%) in Sauton's minimal medium. Quantitation of secreted metabolites with major changes when exposed to (D) acetate (0.2%) (E) glutamate (0.05%) and acetate (0.2%) in Sauton's minimal medium. Means ± SD for triplicate experimental samples. *p < 0.01. Results are representative of at least two independent experiments.

Figure S12. SSA inhibits growth of Mtb. OD₅₈₀ at day 10 of Mtb strains in Sauton's minimal medium containing acetate (0.2%) or glycerol (0.2%) as the sole carbon source with varying amounts of additional succinate semialdehyde. Results are representative of at least two independent experiments.

Figure S13. HOAS activity is dispensable for protection against reactive oxygen intermediates, acid, and starvation. Survival of WT, $\Delta hoas$, $\Delta hoas::hoas$, and $\Delta hoas::E956Ahoas$ after (A) 4-hour exposure to H₂O₂ in 7H9 complete medium, and (B) 6 day incubation in 7H9 complete medium at pH 4.5. (C) Survival of the four strains in PBS with 0.05% tyloxapol detergent. Data are means \pm SD of triplicates in one experiment representative of three.

Figure S14. Rapid Fire Mass spectrometric detection and characterization of HOAS dependent peroxidase. (a) EIC spectra at $m/z = 866.12$ showing succinyl CoA formation in the KGDH reaction progress curve. First 3 sets are standard curve, next 6 sets are KGDH reaction, next 6 sets are reaction without 2-ketoglutarate, and next 6 sets are reaction without tBuOOH. (b) Zoomed in version on the first set of peaks showing time course of reaction progress. First 6 samples are the unactivated and next 6 are the activated reaction. (c) EIC at $m/z = 866.12$ for the Michaelis-Menten kinetics reaction. (d) Zoomed in version on set of peaks (unactivated and activated) obtained with various concentrations of 2-ketoglutarate as indicated.

Figure S15. Kinetic characterization of HOAS dependent peroxidase reaction. Michaelis Menten plot of (a) 2-ketoglutarate for activated (open circles) and unactivated (filled circles) reaction (b) CoA for activated (open circles) and unactivated (filled circles) reaction (c) tBuOOH for activated (open circles) and unactivated (filled circles) reaction. The fitted kinetic parameters are summarized in Table 1. Data points are averages of experimental triplicates and error bars are standard deviations. Solid lines are regression fit to equation 1. Each experiment was repeated at least 3 times.

Figure S16. Rapid Fire Mass spectrometric detection and characterization of AceE peroxidase reaction. (a) EIC spectra at $m/z = 808.12$ showing acetyl CoA formation in the progress curve. First 3 sets are standard curve, next 6 sets are reaction, next 6 sets are reaction without pyruvate, and next 6 sets are reaction without tBuOOH (b) Zoomed in version on the first set of peaks showing time course of reaction progress (c) Comparison of natural abundance isotopic distribution of standard and product. (d) EIC at $m/z = 808.12$ for the Michaelis-Menten kinetics reaction. (e) Zoomed in version on set of peaks obtained with various concentrations of pyruvate as indicated.

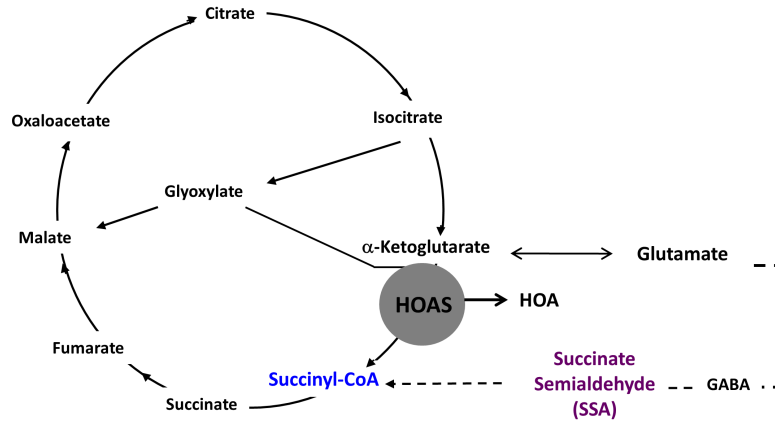
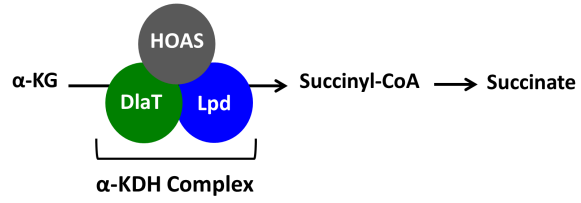
Figure S17. Kinetic characterization of AceE dependent peroxidase reaction. Michaelis Menten plot of (a) pyruvate (b) CoA (c) tBuOOH. The fitted kinetic parameters are summarized in Table 1. Data points are averages of 6 experimental replicates and error bars are standard deviations. Solid lines are regression fit to equation 1. Each experiment was repeated at least 3 times

Figure S1

A.

Mtb genes that encode KDH components
(with HOAS as E1)

Dihydrolipoamide acyltransferase: **DlaT**
Lipoamide dehydrogenase: **Lpd**



B.

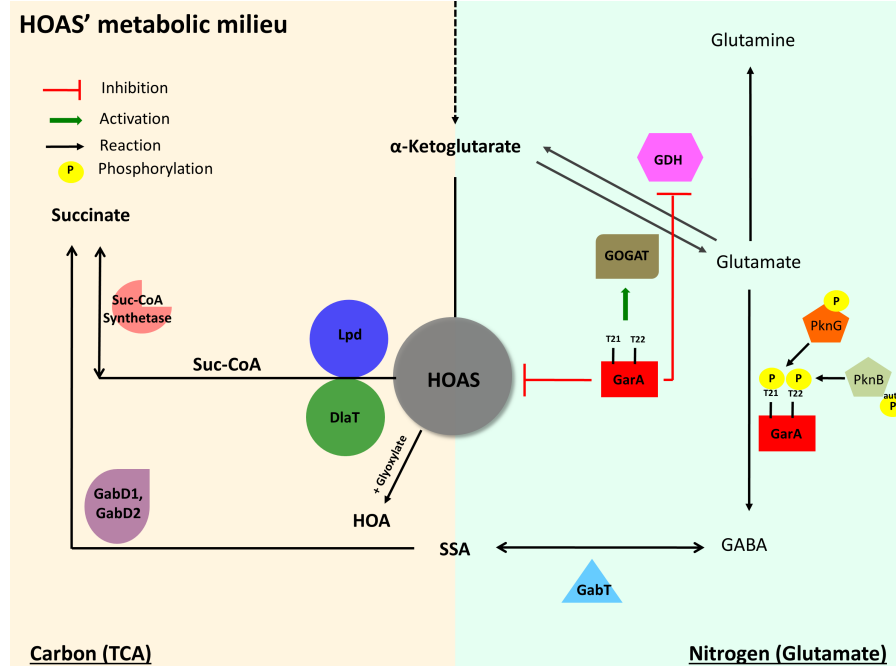
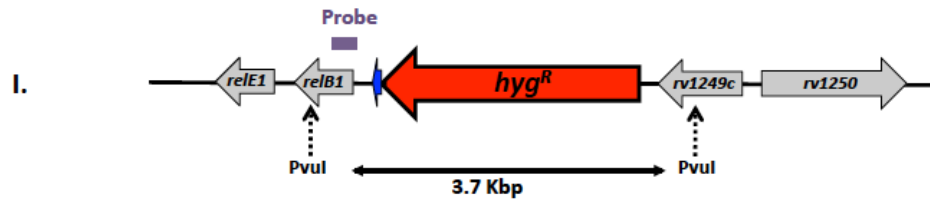


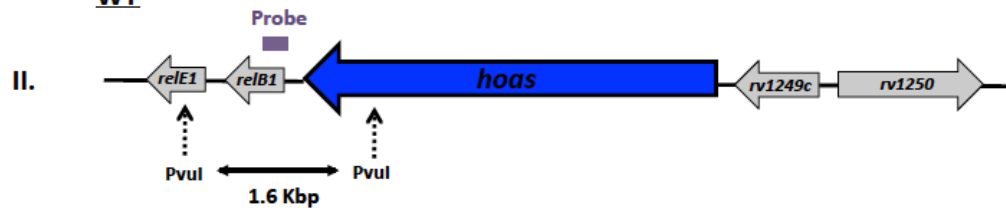
Figure S2

A.

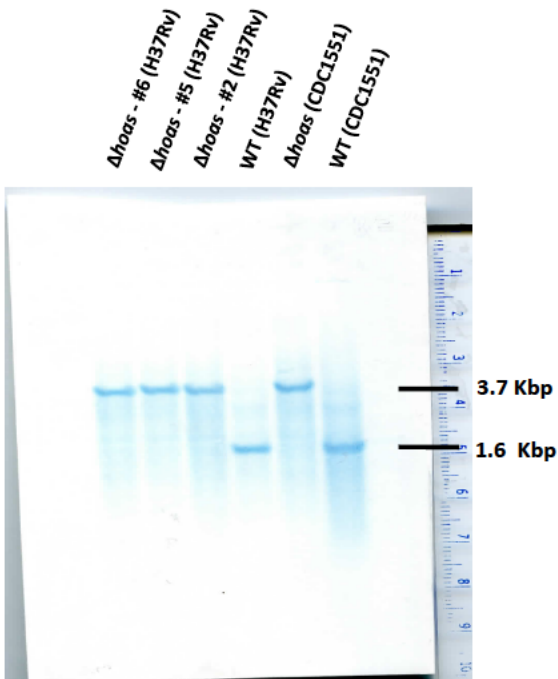
Δhoas



WT



B.



C.

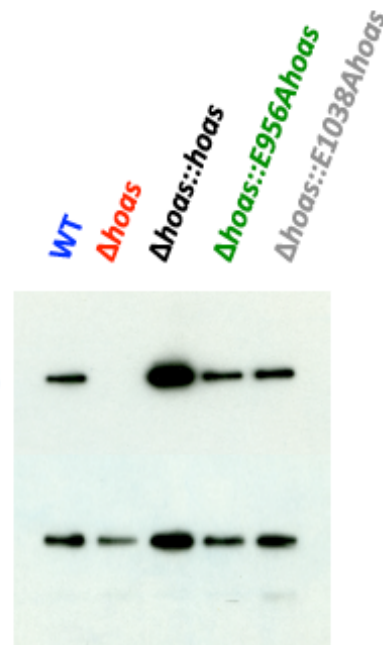
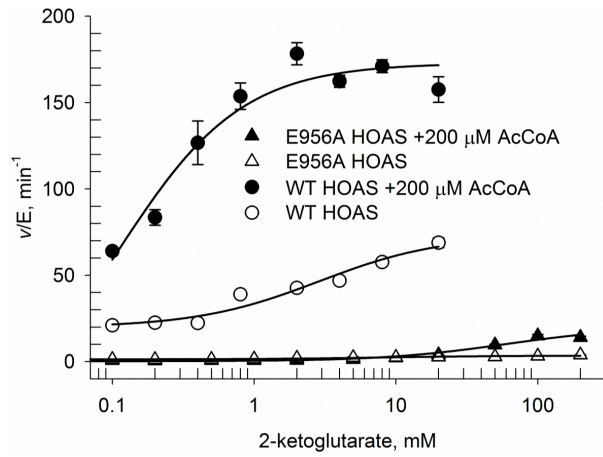


Figure S3

A.



B.

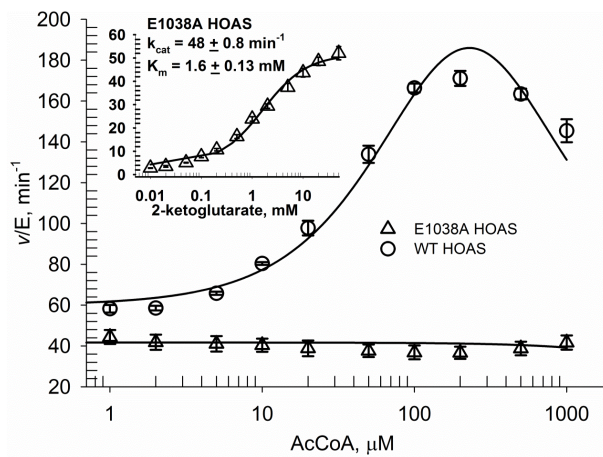
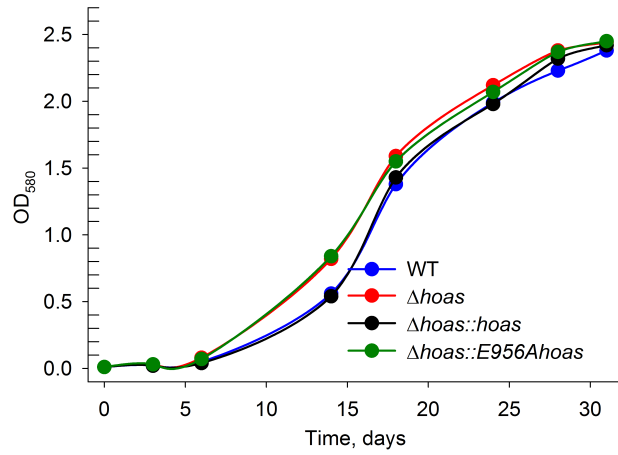


Figure S4

A.



B.

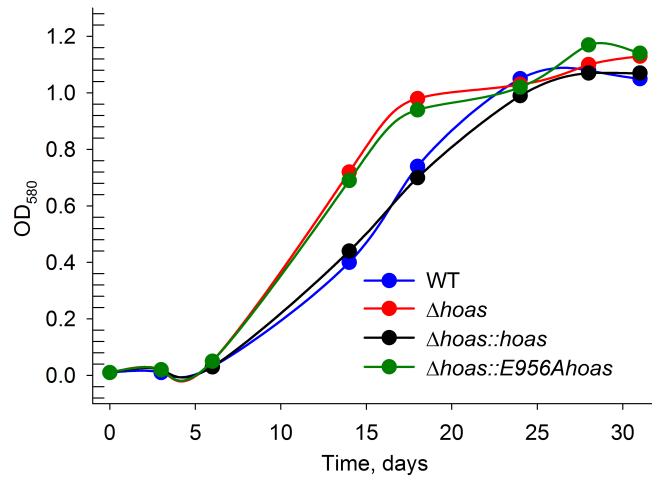
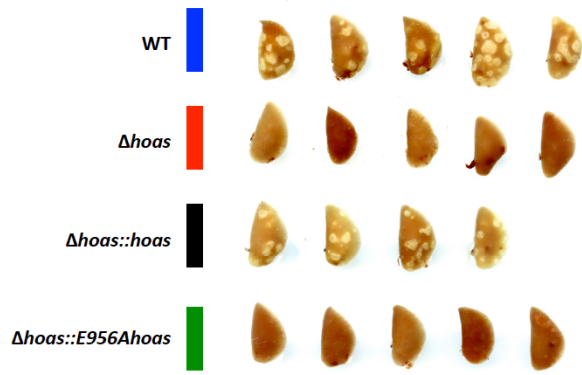


Figure S5

A.



B.

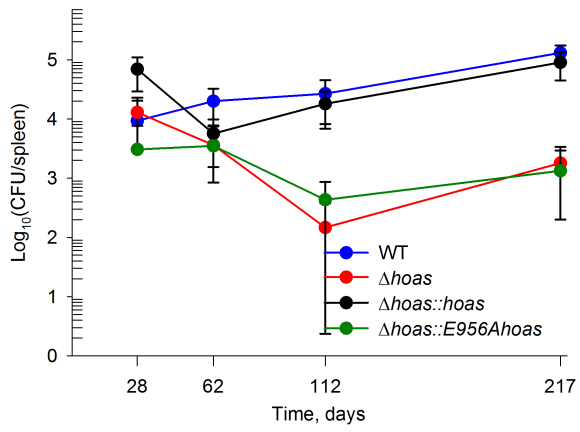
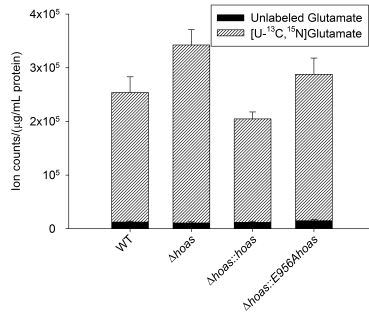


Figure S6

A.



B.

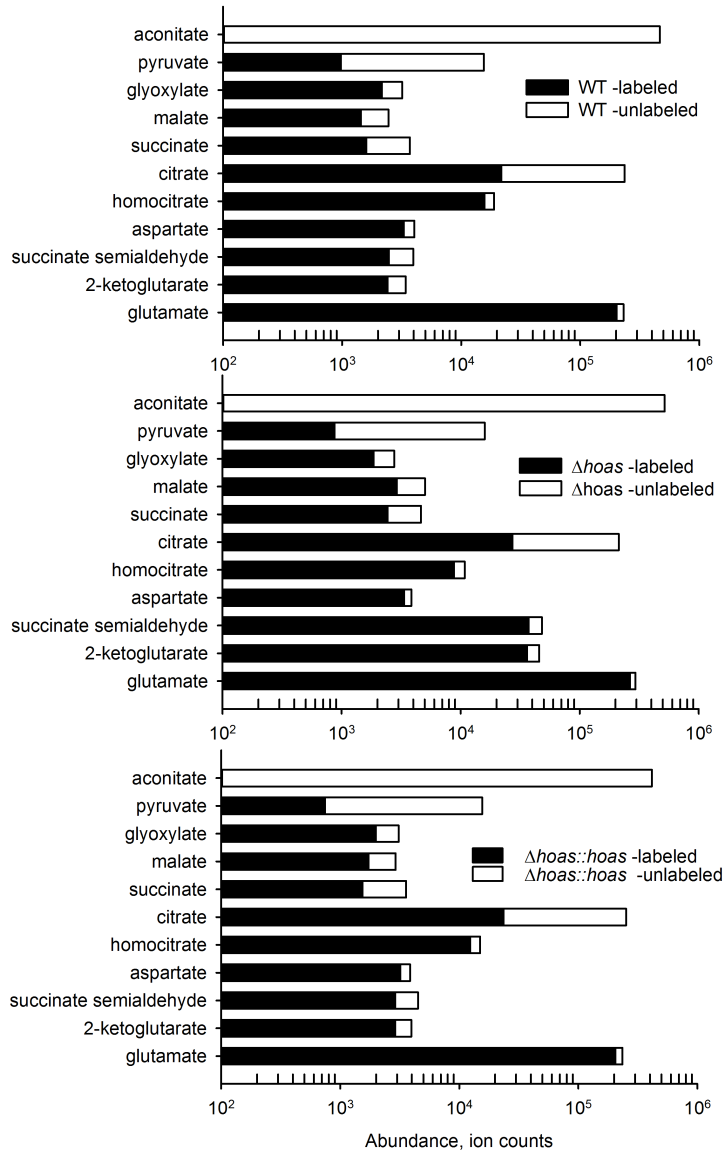
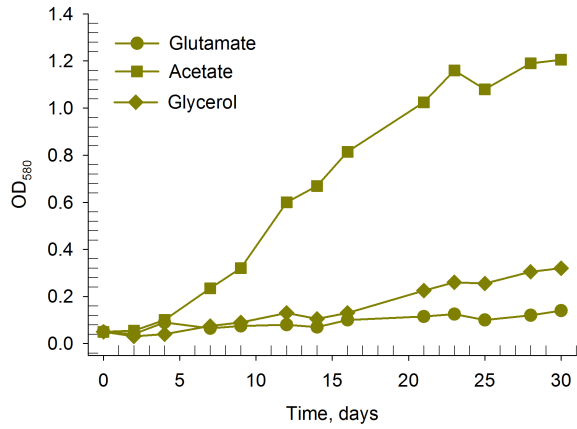
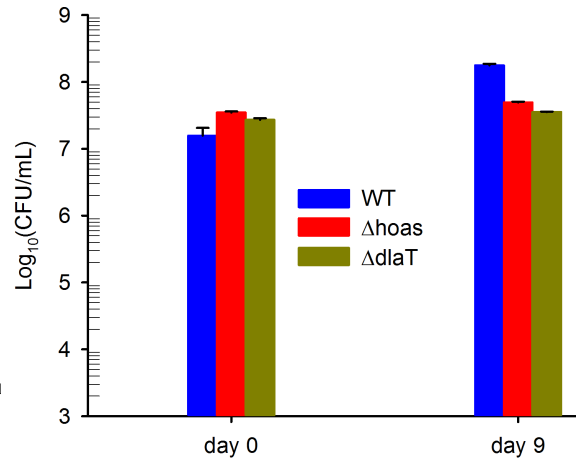


Figure S7

A.



B.



C.

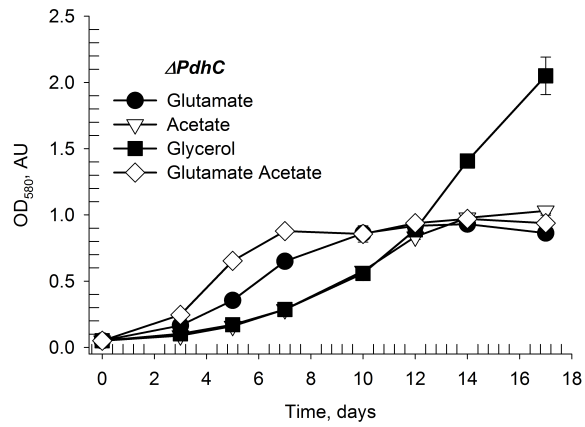
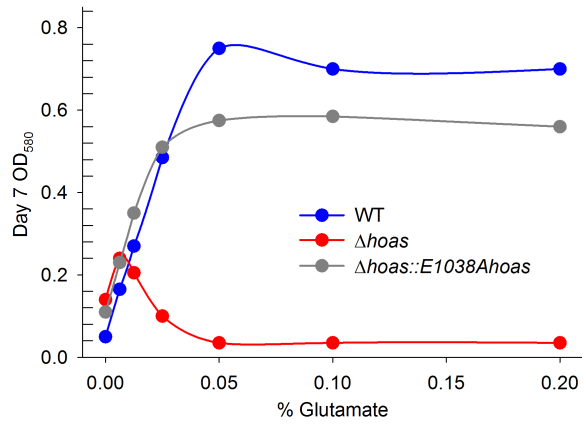


Figure S8

A.



B.

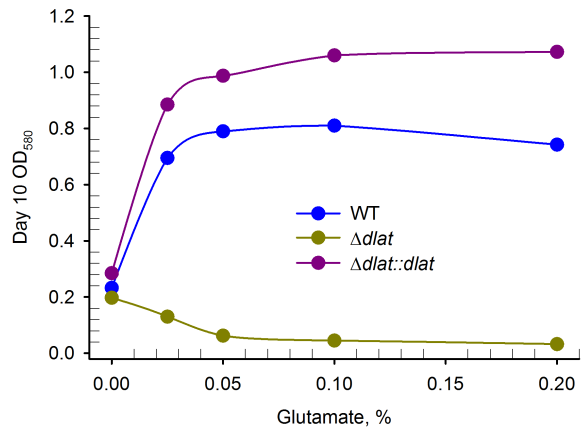


Figure S9

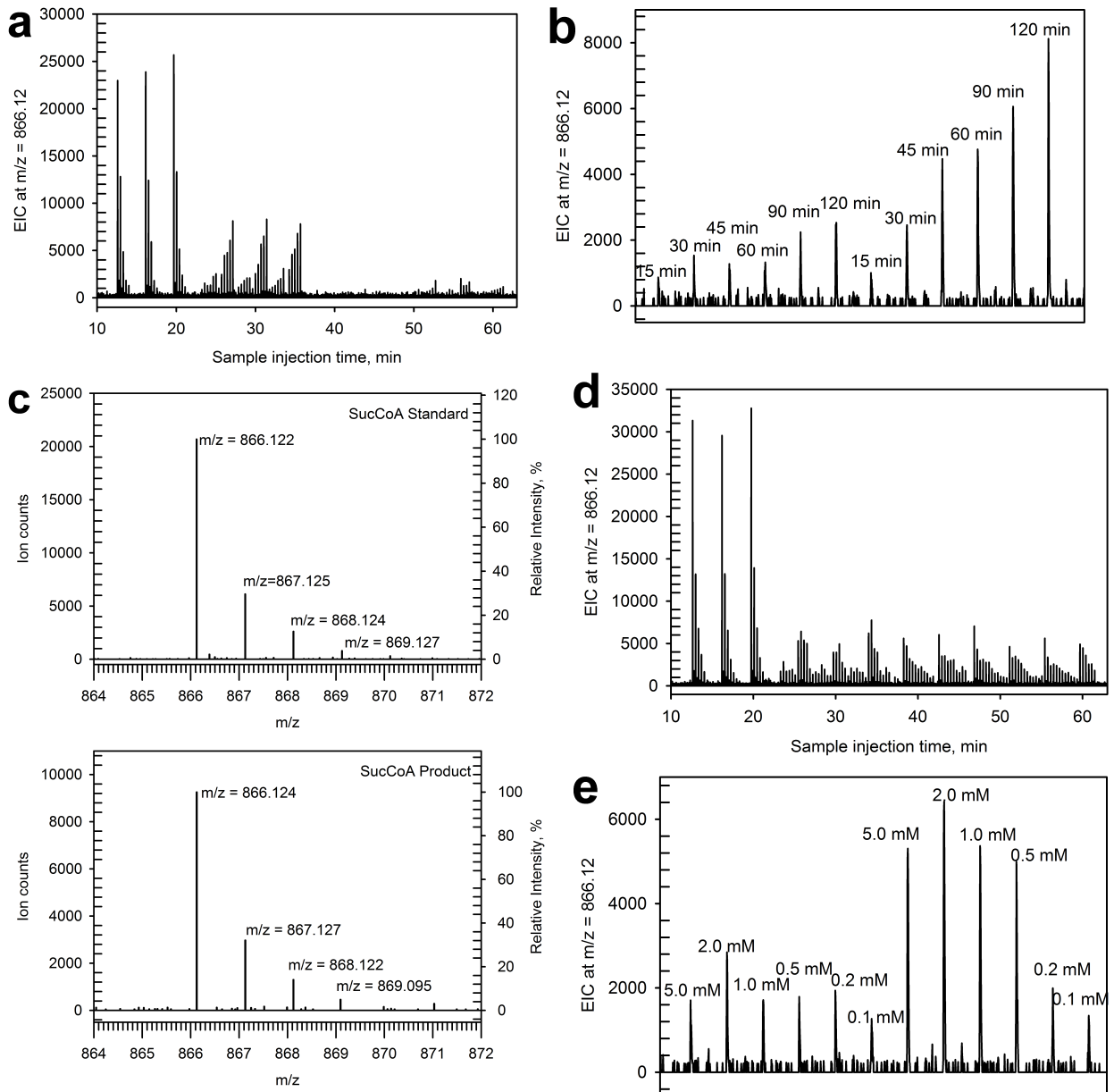


Figure S10

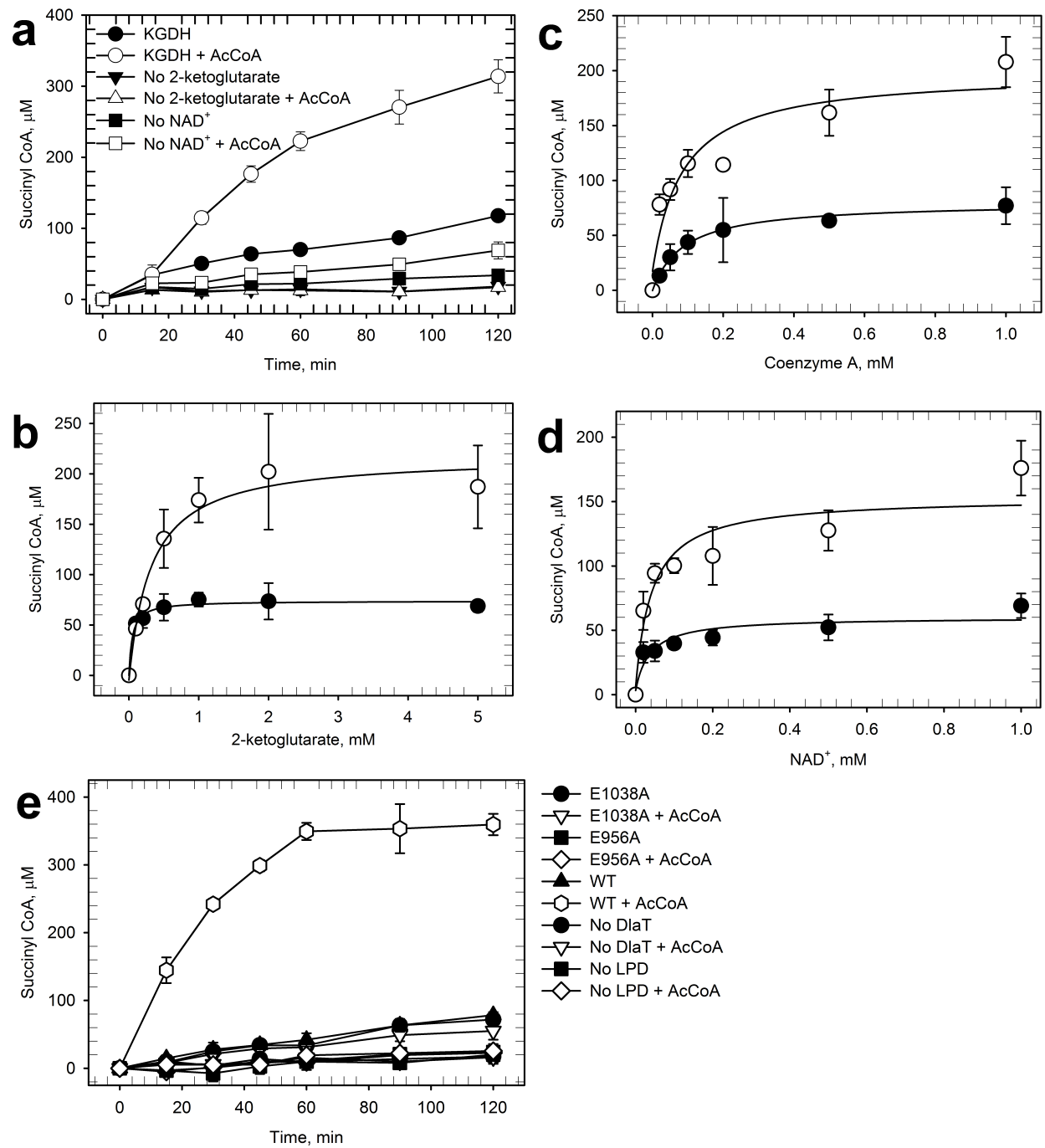
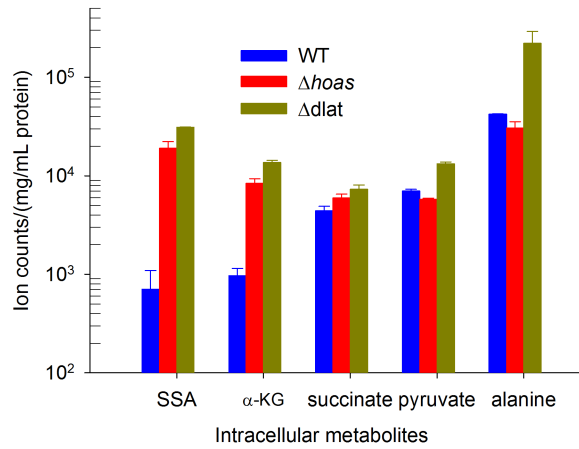
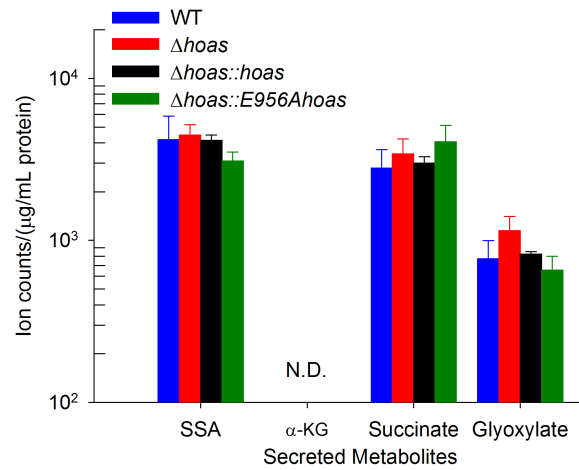


Figure S11

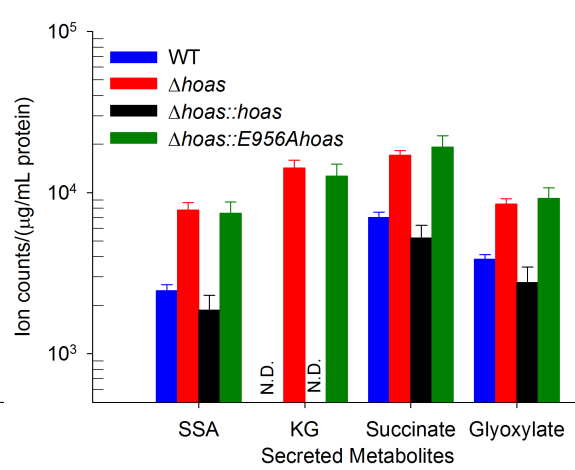
A.



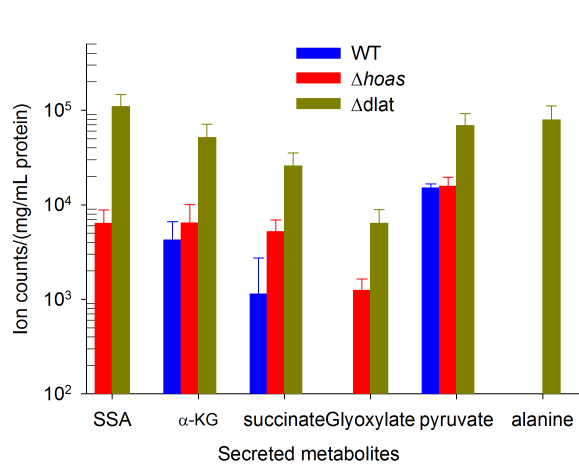
B.



C.



D.



E.

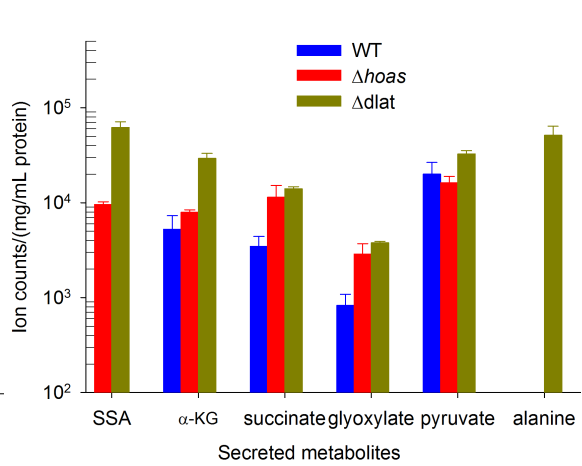


Figure S12

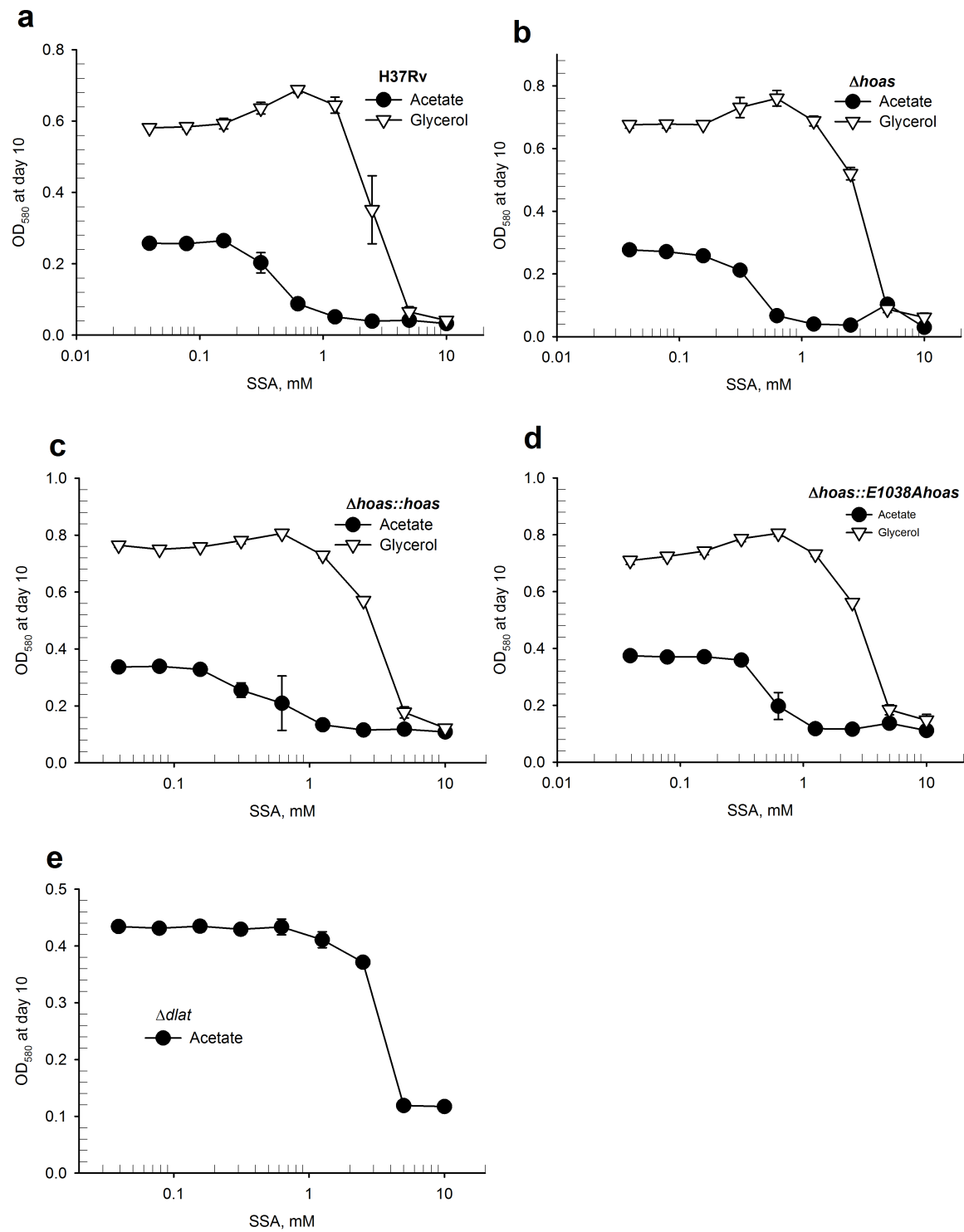
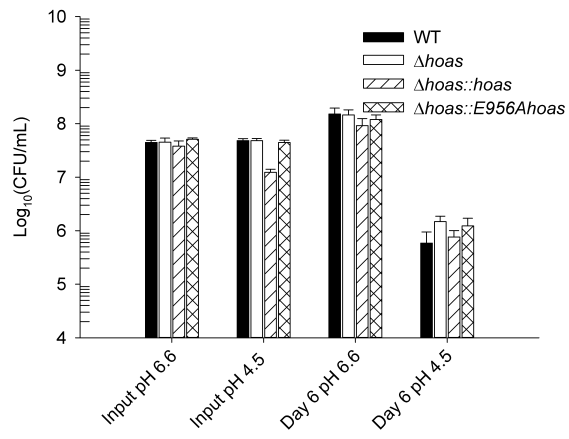
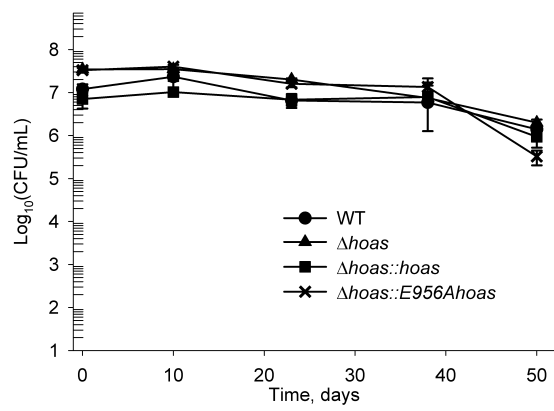


Figure S13

A



B



C

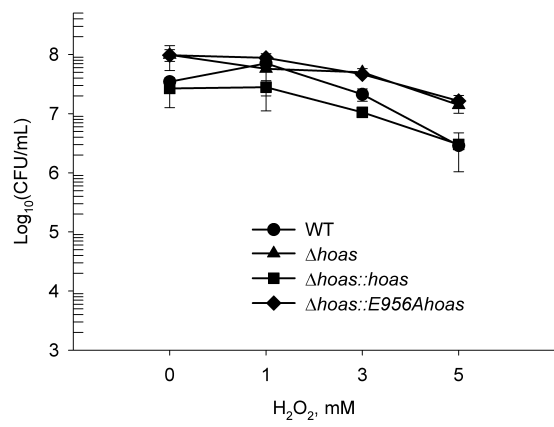


Figure S14

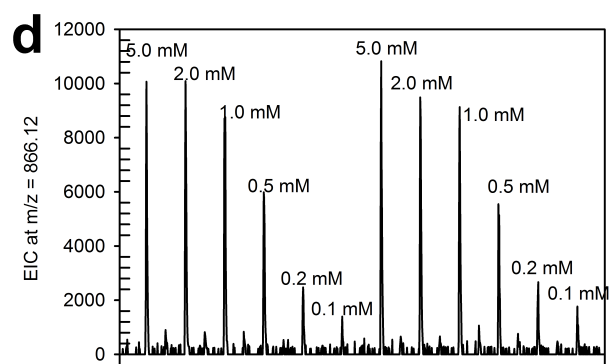
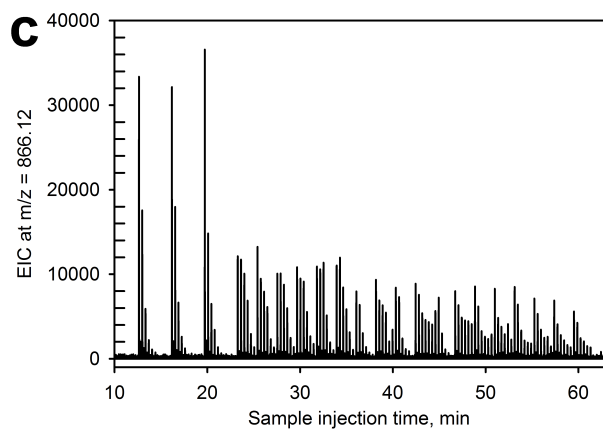
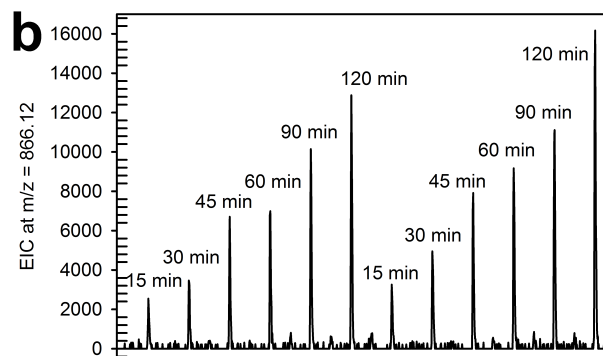
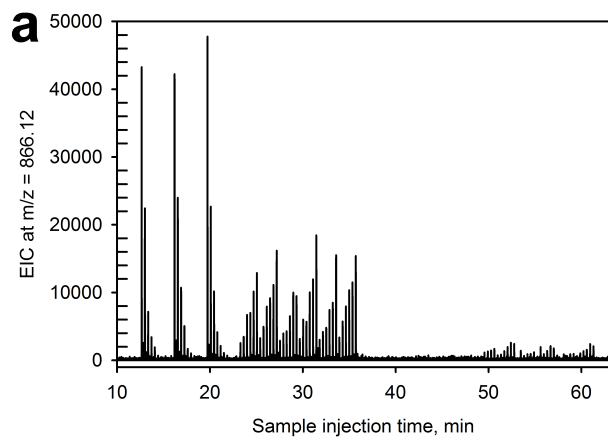


Figure S15

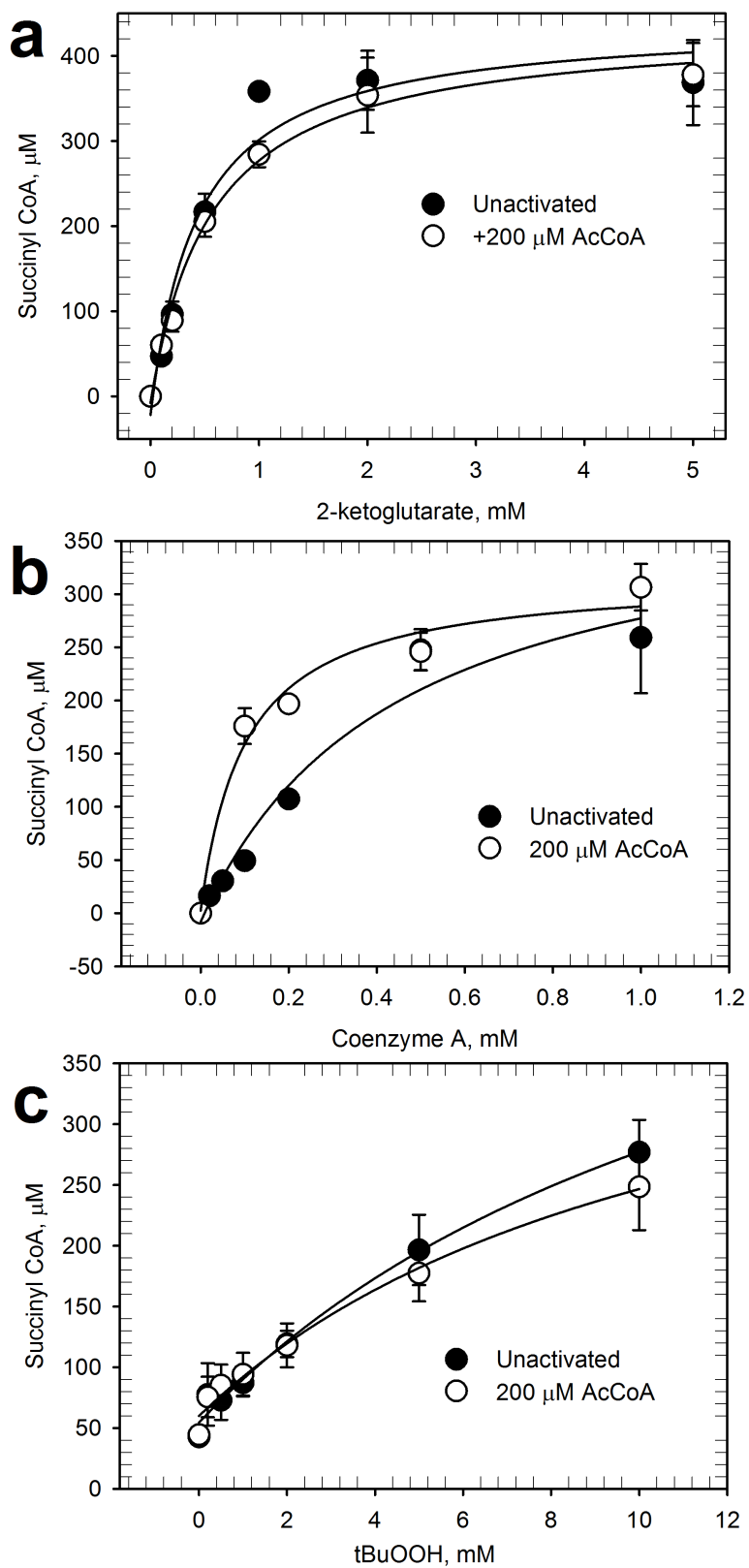


Figure S16

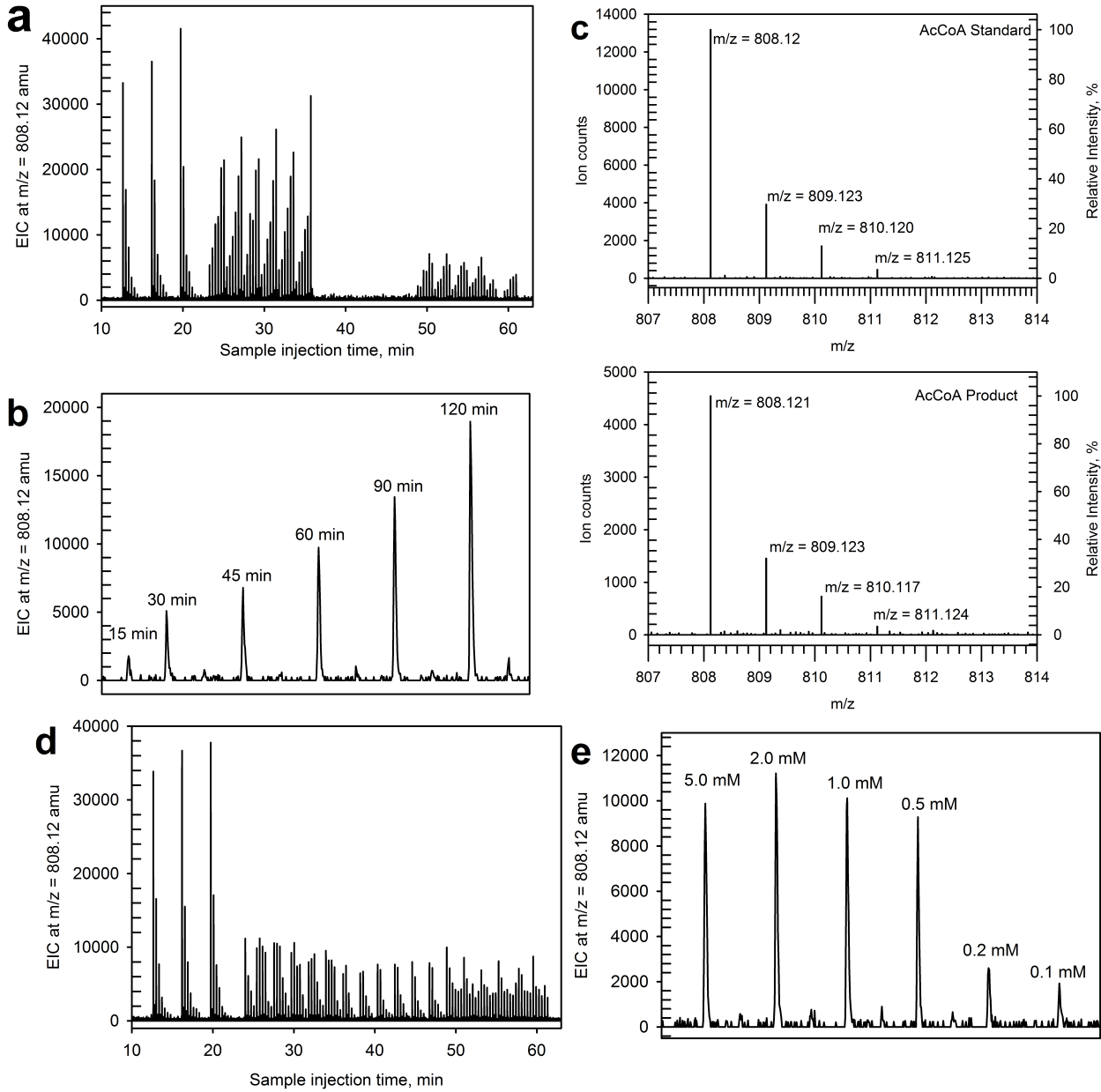


Figure S17

